Journal of Visualization, Vol. 9, No. 4 (2006) 355

# Slamming Simulation

Zibarov, A. V.*, Medvedev, A. V.*, Karpov, A. N.*, Elesin, V. V.*, Orlov, D. A.* and Antonova, A. V.*
* GDT Software Group, Tula, Russia. E-mail: info@cfd.ru, URL: www.cfd.ru
Received 16 November 2006

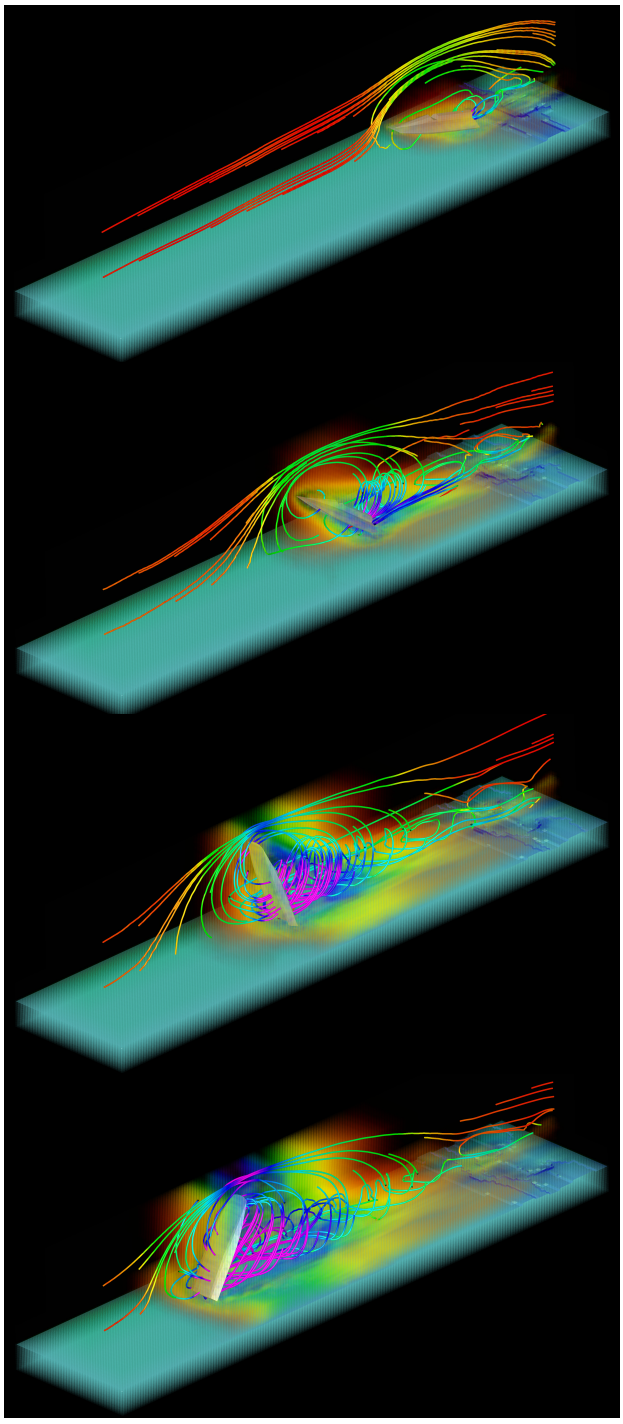


Fig. 1.

These figures show a high speed impact of a boat and wave simulated. The type of the simulation problem is usually solved by Lagrange-Euler approach. The current problem was solved by Sergey A. Sergievskiy from Moscow office of MSC.Software Corporation and visualized using the ScientificVR® package of GDT Software Group, which allows arranging differing visualization techniques simultaneously, namely the semitransparent voxel technique, the semitransparent voxel technique in iso-surface realization and streamlines. Here the semitransparent voxel technique and voxel technique in iso-surface realization present a parameter distribution, such as velocity module distribution of air flowing around the boat and water. The streamlines present vector values of velocity. The voxels, iso-surfaces and streamlines are colored according to a velocity module. The red color is for low module values, and the violet color is for the high ones.

Figure 1(a) shows the moment, when the boat has just passed through the wave. One can see clearly dark blue waves appeared in the place of the passing. The “water-air” interface is presented by light blue voxels in iso-surface realization. Figure 1(b) shows the moment of the first turbulence formation behind the boat, which is caused by a large attack angle of the boat. The turbulence formation is presented by colored voxel graphics and streamlines. Figure 1(c) shows the moment of peak turbulences around the boat, which drives with the attack angle close by the maximum. Figure 1(d) shows the moment of the boat overturning.

Journal of Visualization, Vol. 9, No. 4 (2006) 356

# Visualization Analysis of Large-Scale Three-Dimensional Scalar Data of Ocean Simulation

Furuichi, M.*, Araki, F.* and Sasaki, H.*

* Earth Simulator Center, Japan Agency for Marine-Earth Science and Technology, 3173-25 Showa-machi, Kanazawa-ku, Yokohama-city, Kanagawa 236-0001, Japan.
E-mail: m-furuic@jamstec.go.jp

Received 6 July 2006

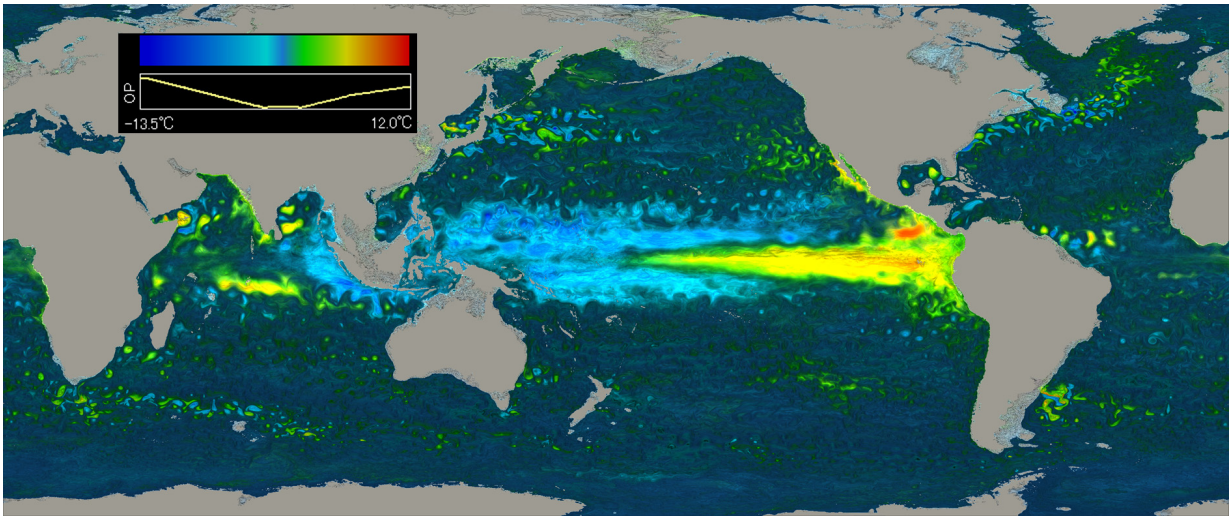


Fig. 1. A snap shot of sea temperature anomalies on 24 Oct 1997. Original size of picture is 3600 × 1500 pixels. El Niño event is captured in the equatorial Pacific Ocean. Indian Ocean Dipole (IOD) is also captured in the Indian Ocean.

We visualize the data set of the hind-cast experiment of OFES (Sasaki et al., 2004). The horizontal resolution and the number of vertical levels are 0.1 degree and 54, respectively. Total data size of simulated sea temperature is 3600 × 1500 × 54 Grids × 4 Bytes × 6575 Snapshots = 7.7 Tera Bytes. In our visualization results, all of the simulated events are displayed by ray-casting volume rendering in the global view like Fig. 1, which represents the IOD and El Niño simultaneously without losing the resolution of original out put data. These sets of the pictures through 54 years must be helpful for understanding the combined influences of the events.

***Reference*** : Sasaki, H., Sasai, Y., Kawahara, S., Furuichi, M., Araki, F., Ishida, A., Yamanaka, Y., Masumoto, Y. and Sakuma, H., A series of eddy-resolving ocean simulations in the world ocean, OFES (OGCM for the Earth Simulator) project, Oceans '04, 3 (2004), 1535-1541.

Journal of Visualization, Vol. 9, No. 4 (2006) 357

# A Novel Molecular Tagging Technique for Simultaneous Measurements of Flow Velocity and Temperature Fields

Hu, H.*[1] and Koochesfahani, M. M.*[2]

*1 Department of Aerospace Engineering, Iowa State University, Ames, Iowa 50011, USA. E-mail: huhui@iastate.edu

*2 Department of Mechanical Engineering, Michigan State University, East Lansing, Michigan 48824, USA. E-mail: koochesf@egr.msu.edu

Received 11 August 2006

(a) Grid image 0.5 ms after the laser excitation pulse.

(b) Same grid 5 ms later.

Fig. 1.

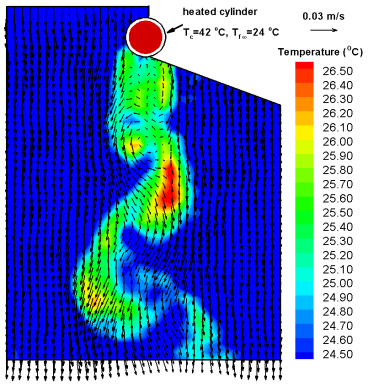


Fig. 2. Simultaneous velocity and temperature fields derived from the image pair shown in Fig. 1.

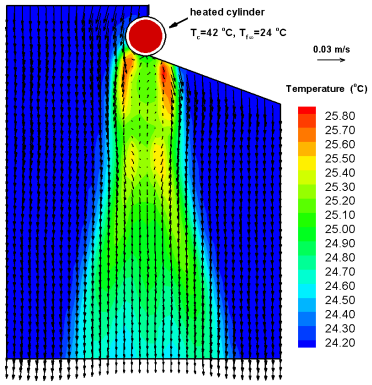


Fig. 3. Ensemble-averaged velocity and temperature fields.

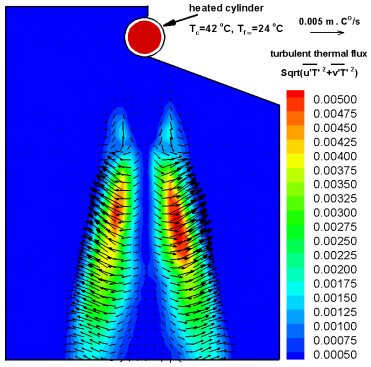


Fig. 4. Measured turbulent thermal flux vectors.

A novel molecule-based flow diagnostic technique, called molecular tagging velocimetry and thermometry (MTV&T), has been developed recently to achieve simultaneous measurements of flow velocity and temperature distributions. For the MTV&T measurements, pulsed laser beams are used to tag phosphorescent tracer molecules premixed in the working flow. The tracer molecules will give off long-lifetime phosphorescence emission, serving as glowing markers for the flow measurements. The movements of the glowing molecules are imaged twice after the same laser pulse. The measured Lagrangian displacements of the tagged molecules between the two interrogations provide the estimates of velocity vectors. Simultaneous temperature measurement is achieved by taking advantage of the temperature dependence of phosphorescence lifetime, which is estimated from the phosphorescence intensity ratio of the two interrogations. An example of the MTV&T measurements taken from a study of the thermal effect on the wake instability behind a heated cylinder is shown here. The molecular tracers are tagged by pulsed multiple laser beams in a grid pattern. Both the initially tagged regions and their subsequent evolution 5 ms later are shown in Fig. 1, along with the resulting simultaneous velocity and temperature distributions derived from the image pair (Fig. 2). Since the instantaneous velocity and temperature distributions are measured simultaneously, ensemble-averaged velocity and temperature fields (Fig. 3) as well as the turbulent thermal flux vectors (Fig. 4), i.e., the correlation between the velocity and temperature fluctuations, can also be derived from the measurements.

# Flow Field Visualization of a Single-Blade Centrifugal Pump Using PIV-Method - Comparison to Numerical Results

Benra, F. -K.*, Dohmen, H. J.* and Sommer, M.*

* University of Duisburg-Essen, Faculty of Engineering Sciences, Institute of Energy and Environmental Engineering, Turbomachinery, 47048 Duisburg, Germany, E-mail: friedrich.benra@uni-due.de

Received 15 August 2006

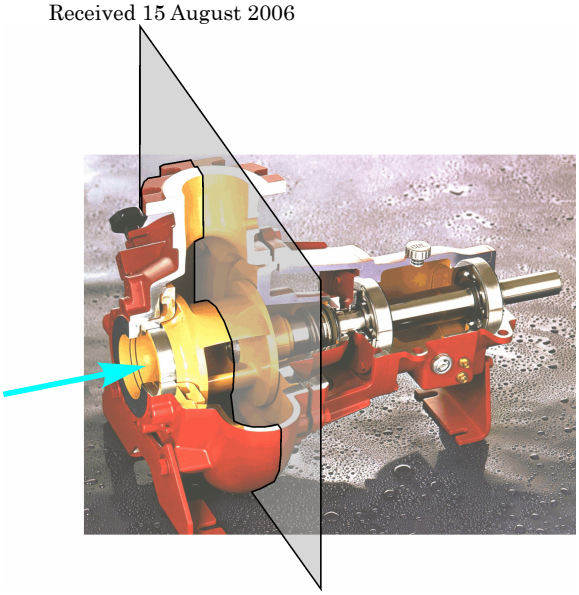

Fig. 1. Single-stage sewage water pump with single-blade Impeller for dry installation with observation plane.

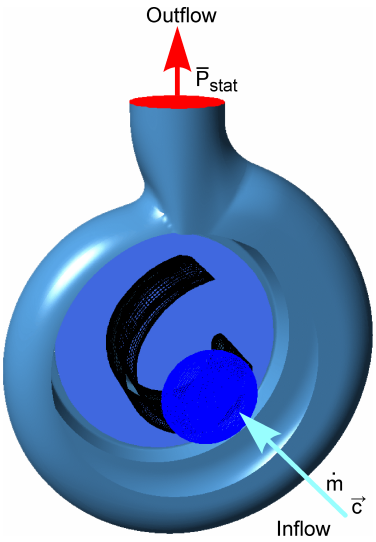


Fig. 2. Computational model of single-blade pump.

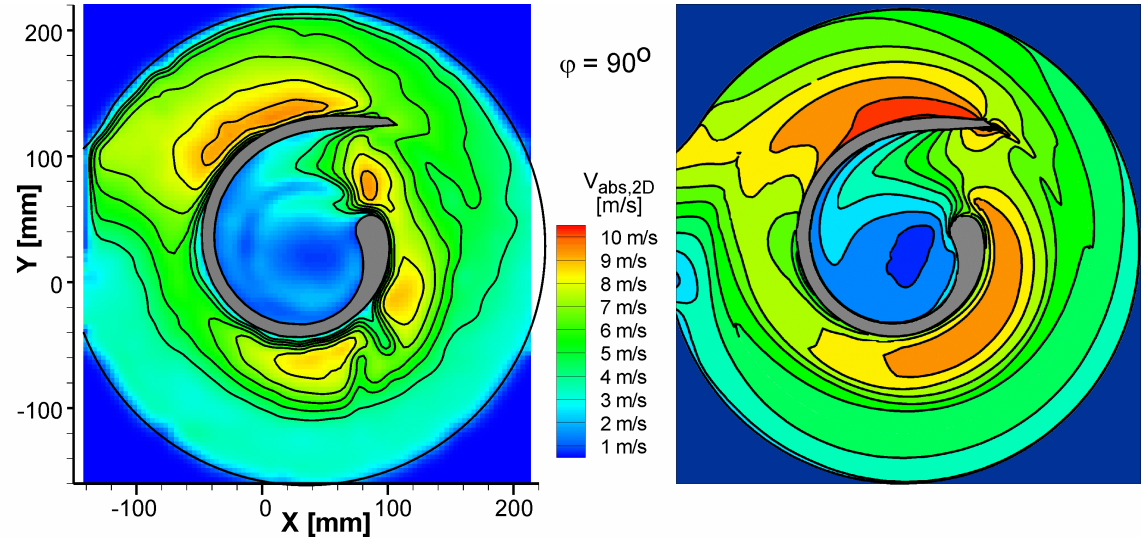


Fig. 3. Comparison of measured (left) and calculated (right) absolute velocity field at design flow conditions at blade position 90 deg.

These figures show the observed geometry and the visualized absolute velocity in the observation plane. The experimental results are obtained by PIV measurements. The calculation is done with a commercial CFD code solving the time dependent Reynolds averaged Navier-Stokes equations (URANS).

# Visualization of Streaks, Thermals and Waves in the Atmospheric Boundary Layer

Fujiyoshi, Y.*[1], Yamashita, K.*[2] and Fujiwara, C.*[2]

*1 Institute of Low Temperature Science, Hokkaido University, N19W8, Sapporo 060-0819, Japan. E-mail: fujiyo@lowtem.hokudai.ac.jp

*2 Graduate School of Environmental Science, Hokkaido University, N10W5, Sapporo 060-0810, Japan.

Received 8 September 2006

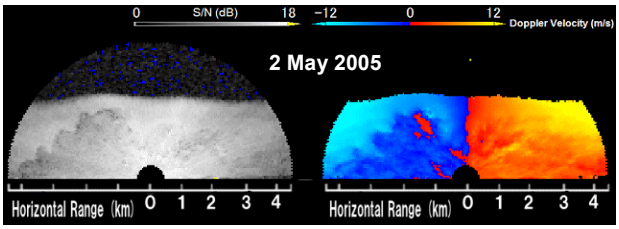


Fig. 1. Vertical cross-sections of back scattering intensity (S/N ratio) and Doppler velocity fields of blue-thermals. Red (blue) colored areas are radial velocities away from (toward) the lidar.

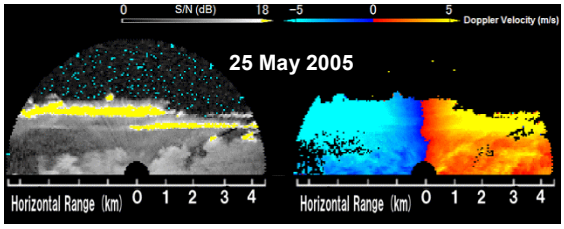


Fig. 2. As Fig. 1, but for moist-thermals developed below the stratus clouds.

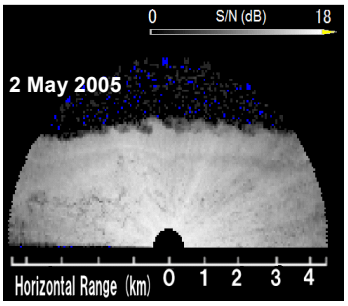


Fig. 3. Vertical cross-section of Kelvin-Helmholtz instability waves developed near the upper boundary of ABL.

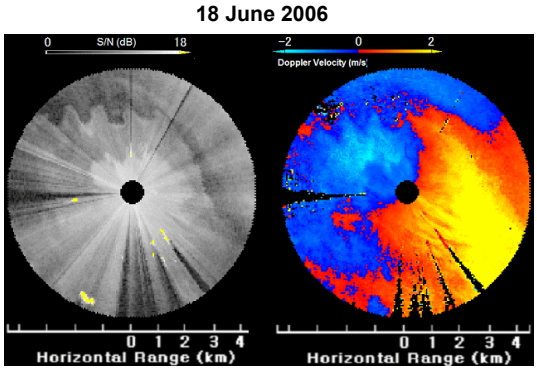


Fig. 4. As Fig.1, but for horizontal cross-sections of waves formed along the horizontal wind shear line.

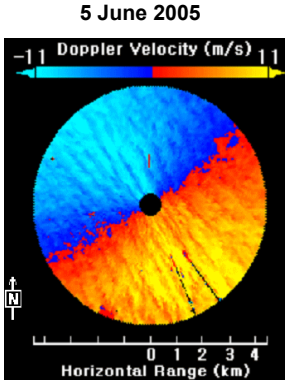


Fig. 5. Doppler velocity fields of streaks formed near the ground surface.

We can visualize the various kinds of atmospheric phenomena that have been hardly seen except for a 3D-Coherent Doppler Lidar with 1.54 μm in wavelength (Mitsubishi Electric Corporation). These figures show several examples of typical organized airflows in the atmospheric boundary layer, that is, thermals (Figs. 1 and 2), Kelvin-Helmholtz instability waves (Fig. 3), waves developed along the horizontal wind shear zone (Fig. 4) and streaks (Fig. 5).

Journal of Visualization, Vol. 9, No. 4 (2006) 360

# Visualization of Kelvin waves activity in the hollow vortex

Vatistas, H. G.* and Ait Abderrahmane, H.*
*Department of Mechanical and Industrial Engineering University of Concordia
Montreal 1455 de Maisonneuve Blvd. West Montreal, Quebec, H3G 1M8, CANADA.
Received 15 September 2006

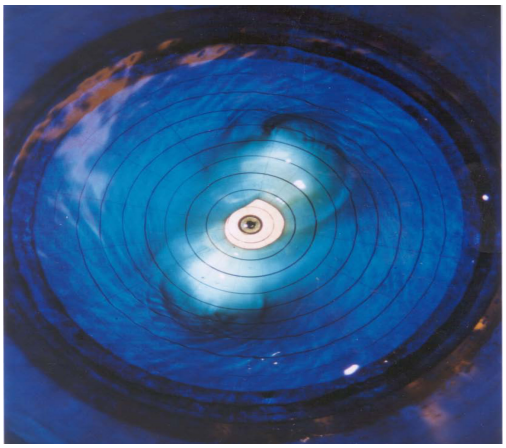

Mode 2 of Kelvin's equilibria

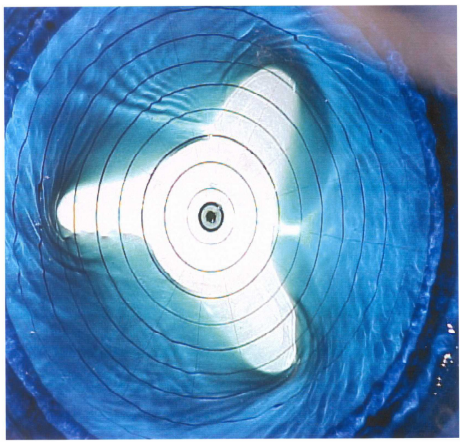

Mode 3 of Kelvin's equilibria

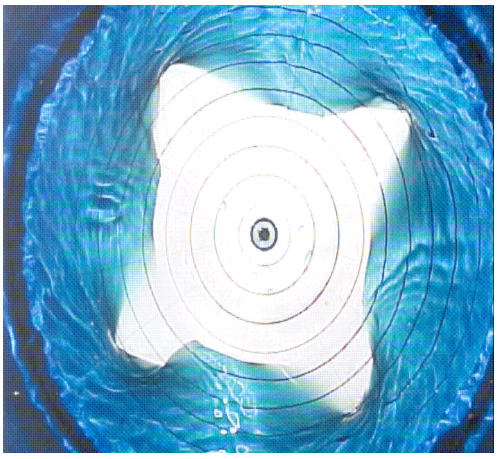

Mode 4 of Kelvin's equilibria

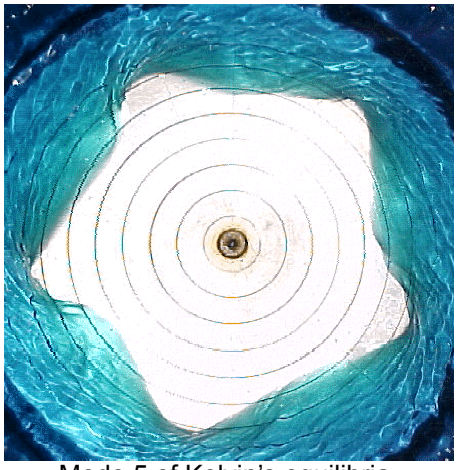

Mode 5 of Kelvin's equilibria

The figures above bring into view the wave activity in a hollow vortex generated under shallow water conditions within a cylindrical container with a flat disk rotating (in counter-clockwise direction) near the bottom. The diameters of the container and the flat disk were 285 mm and 252 mm respectively, whereas the initial height of the water was 27 mm. Depending on the angular velocity of the disk stationary Kelvin modes (Kelvin's equilibria) ranging from two to six were observed (here we only show up to five). The range of disk speed where the equilibria existed became narrower as the wave number increased. These vortex patterns were made visible via a blue water soluble dye. The ratio of the celerity of the modes to the angular velocity of the disk decreases linearly. The figures also show an additional wave activity, manifested by shaded ripples travelling along with the basic patterns. Two kinds of ripples, similar to those generated by ships, were observed. Coalescent (compression*) waves were detected ahead of the main pattern while the refraction (expansion) type, was found to develop behind the pattern.

*In the gas dynamic analogous system